European Journal of Medicinal Chemistry 92 (2015) 212–220

Contents lists available at ScienceDirect

European Journal of Medicinal Chemistry

journal homepage: http://www.elsevier.com/locate/ejmech

Original article

Synthesis, anticancer activity and molecular docking studies on a series of heterocyclic *trans*-cyanocombretastatin analogues as antitubulin agents

Narsimha Reddy Penthala [a], Hongliang Zong [b], Amit Ketkar [c], Nikhil Reddy Madadi [a], Venumadav Janganati [a], Robert L. Eoff [c], Monica L. Guzman [b], Peter A. Crooks [a, *]

[a] Department of Pharmaceutical Sciences, College of Pharmacy, University of Arkansas for Medical Sciences, Little Rock, AR 72205-7199, USA
[b] Division of Hematology/Oncology, Department of Medicine, Weill Cornell Medical College, New York, NY 10021, USA
[c] Department of Biochemistry and Molecular Biology, University of Arkansas for Medical Sciences, Little Rock, AR 72205-7199, USA

ARTICLE INFO

Article history:
Received 16 August 2014
Received in revised form
21 November 2014
Accepted 28 December 2014
Available online 29 December 2014

Keywords:
Trans-cyanocombretastatin analogues
Anti-cancer activity
Leukemia cell lines
Molecular docking
Tubulin binding

ABSTRACT

A series of heterocyclic combretastatin analogues have been synthesized and evaluated for their anticancer activity against a panel of 60 human cancer cell lines. The most potent compounds were two 3,4,5-trimethoxy phenyl analogues containing either an (*Z*)-indol-2-yl (**8**) or (*Z*)-benzo[*b*]furan-2-yl (**12**) moiety; these compounds exhibited GI_{50} values of <10 nM against 74% and 70%, respectively, of the human cancer cell lines in the 60-cell panel. Compounds **8**, and **12** and two previously reported compounds in the same structural class, i.e. **29** and **31**, also showed potent anti-leukemic activity against leukemia MV4-11 cell lines with LD_{50} values = 44 nM, 47 nM, 18 nM, and 180 nM, respectively. From the NCI anti-cancer screening results and the data from the *in vitro* toxicity screening on cultured AML cells, seven compounds: **8**, **12**, **21**, **23**, **25**, **29** and **31** were screened for their *in vitro* inhibitory activity on tubulin polymerization in MV4-11 AML cells; at 50 nM, **8** and **29** inhibited polymerization of tubulin by >50%. The binding modes of the three most active compounds (**8**, **12** and **29**) to tubulin were also investigated utilizing molecular docking studies. All three molecules were observed to bind in the same hydrophobic pocket at the interface of α- and β-tubulin that is occupied by colchicine, and were stabilized by van der Waals' interactions with surrounding tubulin residues. The results from the tubulin polymerization and molecular docking studies indicate that compounds **8** and **29** are the most potent anti-leukemic compounds in this structural class, and are considered lead compounds for further development as anti-leukemic drugs.

1. Introduction

A variety of natural products has been isolated from the bark of the South African tree *Combretum caffrum* which includes the combretastatins [1,2]. Combretastatins (Fig. 1, **I** and **II**) have been shown to be cytotoxic, with combretastatin A-4 (CA-4, Fig. 1, **I**) being the most potent [3,4]. CA-4 inhibits tubulin polymerization, and competitively inhibits the binding of radiolabeled colchicines to tubulin. CA-4 also exhibits potent cytotoxicity against a variety of cancer cell lines, and has been shown to be active against multidrug resistant (MDR) cancer cell lines [5–7].

Structurally related cyanocombretastatin analogues [8,9] (Fig. 1, **III**) and similar analogues that incorporate different heterocyclic moieties, such as indole, benzothiophene, quinoline and quinazoline have also been reported as cytotoxic compounds, and are potent inhibitors of tubulin polymerization potencies comparable to that of CA-4 [10–13]. In this respect, the 3,3-diarylacrylonitrile analog CC-5079 has been reported as a novel synthetic tubulin polymerization inhibitor with potential use in cancer chemotherapy [14] and 2,3-diarylacrylonitriles have emerged as important synthons for the synthesis of a wide spectrum of biologically active molecules [15]. Such compounds have been shown to possess spasmolytic, estrogenic, hypotensive, antioxidant, tuberculostatic, antitrichomonal, and insecticidal properties [16].

Many natural medicinal agents, such as the combretastatins, the colchicines (Fig. 1, **IV**), and the podophyllotoxins, possess a

* Corresponding author.
E-mail address: pacrooks@uams.edu (P.A. Crooks).

http://dx.doi.org/10.1016/j.ejmech.2014.12.050
0223-5234/© 2014 Published by Elsevier Masson SAS.

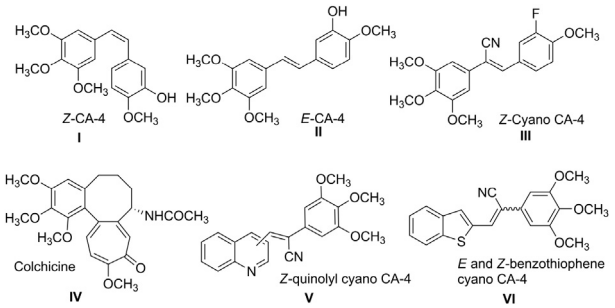

Fig. 1. Chemical structures of potent antitubulin agents.

trimethoxyphenyl moiety in their structure. The cytotoxic properties of such compounds are believed to be related to their anti-tubulin properties [17–21]. A large number of CA-4 derivatives have been synthesized and evaluated for anti-tubulin activity [22–29]. SAR studies have revealed that a 3′,4′,5′-trimethoxyphenyl moiety and a *cis*-configuration of the olefinic bond in these compounds are essential structural elements for biological activity [30,31]. The presence of the *cis*-ethylene bridge that connects the two aryl rings (two planar rings tilted at 50–60^0 to each other [1,31]) is believed to be the key structural factor that holds these structural moieties at an appropriate distance apart, to maintain the correct dihedral angle that maximizes interaction with the colchicine binding site on tubulin protein [32]. We have recently reported on the synthesis and anti-cancer activities of a series of (*Z*)-quinolinylcyano- (**V**) and (*E*)- and (*Z*)-benzothiophene cyano-combretastatin analogues (Fig. 1, **VI**) [11,12], and have determined that such analogues (e.g. compound **29**, Fig. 2) appear to overcome cell-associated P-glycoprotein (P-gp)-mediated resistance in tumor cells, since they are equipotent in inhibiting both OVCAR8 and NCI/ADR-RES cell growth [11].

Previous studies on combretastatin analogues have shown that replacement of the 3-hydroxy-4-methoxyphenyl moiety of CA-4 with heterocyclic groups such as quinoline, quinazoline and benzothiophene results in improved anti-cancer activity [11,12,33]. In the present work, we have synthesized a variety of heterocyclic (*Z*)-cyanocombretastatin analogues that incorporate 2- and 3-indolyl, 2- and 3-benzofuranyl, 2-benzothiophenyl, and 2-benzothiazolyl moieties as replacements for the 3-fluoro-4-methoxyphenyl group in (*Z*)-cyano CA-4 [9] (Fig. 1, **III**).

2. Results and discussion

2.1. Drug synthesis

(*Z*)-Indol-2-yl cyanocombretastatin analogues (**8**–**11**), (*Z*)-benzo[*b*]furan-2-yl cyanocombretastatin analogues (**12**–**14**) and (*Z*)-benzo[*d*]thiazol-2-yl cyanocombretastatin analogues (**15**–**17**) were synthesized by refluxing the appropriate indole-2-carbaldehyde (**1**), 4-cyanobenzyl substituted indole-2-carbaldehyde (**2**), benzo[*b*]furan-2-carbaldehyde (**3**) or benzo[*d*]thiazole-2-carbaldehyde (**4**) with a variety of phenylacetonitriles, i.e., 3,4,5-trimethoxyphenylacetonitrile (**5**), 3,4-dimethoxyphenyl acetonitrile (**6**), and 3,5-dimethoxyphenyl acetonitrile (**7**), in 5% sodium methoxide/methanol (Scheme 1). Confirmation of the structure and purity of these analogues was obtained from ^{1}H NMR, ^{13}C NMR and high resolution mass spectroscopic analysis. The geometry of the double bond (*E*- or *Z*-configuration) in these molecules was established as the (*Z*)-isomer from single crystal X-ray crystallographic data [34,35].

A second series of indole-3-yl (**21**–**24**), and (*Z*)-benzo[*b*]furan-3-yl cyanocombretastatin analogues (**25**–**27**) were synthesized by refluxing a variety of indole-3-carbaldehydes (**18**–**19**) or benzo[*b*]furan-3-carbaldehyde (**20**) with appropriate phenylacetonitriles (**5**–**7**) in 5% sodium methoxide/methanol (Scheme 2).

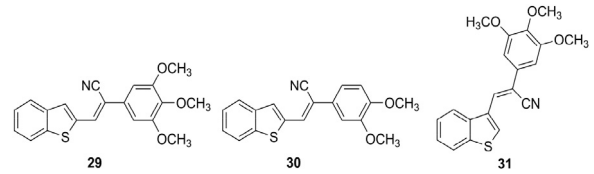

Fig. 2. *Z*-Benzo[*b*]thiophen-2-yl cyanocombretastatin analogues (**29**–**31**) [11].

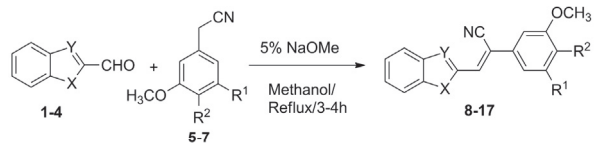

1: X=NH, Y=CH; **2**: X=*N*-CH$_2$-4-CN-C$_6$H$_4$ Y=CH
3: X=O, Y=CH; **4**: X=S, Y= N

Compound	X	Y	R^1	R^2
8	NH	CH	-OCH$_3$	-OCH$_3$
9	NH	CH	H	-OCH$_3$
10	NH	CH	-OCH$_3$	H
11	-*N*-CH$_2$-C$_6$H$_4$-*p*-CN	CH	-OCH$_3$	-OCH$_3$
12	O	CH	-OCH$_3$	-OCH$_3$
13	O	CH	H	-OCH$_3$
14	O	CH	-OCH$_3$	H
15	S	N	-OCH$_3$	-OCH$_3$
16	S	N	H	-OCH$_3$
17	S	N	-OCH$_3$	H

Scheme 1. Synthesis of (*Z*)-indol-2-yl, (Z)-benzo[*b*]furan-2-yl, and (Z)-benzo[*d*] thiazol-2-yl acrylonitriles (**8**–**17**).

2.2. Biological evaluation

2.2.1. In vitro growth inhibition and cytotoxicity

All compounds were evaluated for their cytotoxic potency in a preliminary screen against a panel of 60 human cancer cell lines (NCI-60 panel) at a single analogue concentration (10^{-5} M). The 60 cell line panel is organized into subpanels representing leukemia, non-small cell lung, colon, central nervous system, melanoma,

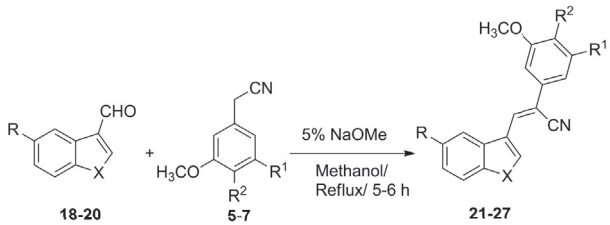

18: X=NH, R=H
19: X=NH, R=-OCH$_3$
20: X=O, R=H

Compound	X	R	R^1	R^2
21	NH	H	-OCH$_3$	-OCH$_3$
22	NH	H	H	-OCH$_3$
23	NH	H	-OCH$_3$	-H
24	NH	OCH$_3$	-OCH$_3$	-OCH$_3$
25	O	H	-OCH$_3$	-OCH$_3$
26	O	H	H	-OCH$_3$
27	O	H	-OCH$_3$	H

Scheme 2. Synthesis of (*Z*)-indole-3-yl, and (*Z*)-benzo[*b*]furan-3-yl cyanocombretastatins (**21**–**27**).

Table 1
Growth inhibition (GI_{50}/μM)[a] data for (*Z*)-indol-2-yl (**8 11**), (*Z*)-benzo[*b*]furan-2-yl (**12**, **13**), and (*Z*)-benzo[*d*]thiazol-2-yl (**15 17**) cyano combretastatin analogues.

Panel/cell line	**8**	**9**	**11**	**12**	**13**	**15**	**17**
	μM	μM	μM	μM	μM	μM	μM
Leukemia							
CCRF-CEM	0.017	0.062	0.136	0.024	0.777	0.055	na
HL-60(TB)	<0.01	0.034	0.031	<0.01	0.481	0.066	0.345
K-562	<0.01	0.039	0.039	<0.01	0.467	0.051	0.333
MOLT-4	0.023	0.084	0.274	0.047	0.548	9.20	3.38
RPMI-8226	<0.01	0.151	0.199	0.019	1.32	0.237	2.29
SR	<0.01	0.042	na	<0.01	0.470	0.107	0.402
Lung cancer							
A549/ATCC	<0.01	0.114	0.076	<0.01	0.520	0.379	na
EKVX	1.16	0.307	na	0.059	na	na	na
HOP-62	<0.01	na	0.092	<0.01	2.29	1.93	3.35
HOP-92	<0.01	0.058	0.077	<0.01	1.13	nd	0.534
NCI-H226	<0.01	0.399	14.5	<0.01	34.5	0.844	4.11
NCI-H23	<0.01	0.236	0.246	<0.01	3.11	3.25	2.84
NCI-H322M	nd	0.735	0.465	<0.01	6.18	2.29	>10.0
NCI-H460	<0.01	0.053	0.093	<0.01	0.472	0.336	2.86
NCI-H522	<0.01	0.049	0.033	<0.01	0.438	0.022	na
Colon cancer							
COLO 205	0.016	0.232	0.097	<0.01	0.404	0.036	0.574
HCC-2998	0.018	0.366	0.265	0.01	2.33	0.297	8.39
HCT-116	<0.01	0.044	0.047	<0.01	0.418	0.052	0.404
HCT-15	<0.01	0.048	0.089	<0.01	0.469	0.045	0.414
HT29	<0.01	0.048	0.048	<0.01	0.373	0.037	0.438
KM12	<0.01	0.076	0.047	<0.01	0.356	0.278	2.01
SW-620	<0.01	0.042	0.048	<0.01	0.388	0.038	0.343
CNS Cancer							
SF-268	0.015	1.48	0.086	0.247	2.05	1.03	3.09
SF-295	<0.01	0.036	0.037	<0.01	0.708	0.508	2.46
SF-539	<0.01	0.047	0.039	<0.01	1.56	0.097	1.68
SNB-19	<0.01	0.189	0.085	<0.01	5.55	2.49	>10.0
SNB-75	<0.01	0.036	0.039	<0.01	1.78	0.145	2.13
U251	<0.01	0.075	0.044	<0.01	0.760	1.65	1.91
Melanoma							
LOX IMVI	<0.01	0.064	0.090	<0.01	0.930	0.073	1.84
MALME-3M	8.28	nd	nd	59.9	0.629	0.515	0.699
M14	<0.01	0.039	0.056	<0.01	0.437	0.193	1.21
MDA-MB-435	<0.01	0.021	0.024	<0.01	0.229	0.021	0.199
SK-MEL-2	<0.01	0.312	0.528	<0.01	0.487	0.287	0.958
SK-MEL-28	na	1.94	0.161	<0.01	3.51	1.81	1.98
SK-MEL-5	<0.01	0.142	0.060	<0.01	0.564	0.100	1.37
UACC-257	1.06	27.0	0.062	63.2	18.0	>100	na
UACC-62	<0.01	0.038	0.058	<0.01	0.557	0.052	0.755
Ovarian cancer							
IGROV1	<0.01	0.482	0.183	0.022	1.27	1.27	0.706
OVCAR-3	<0.01	0.034	0.042	<0.01	0.279	0.031	0.285
OVCAR-4	15.2	0.735	0.672	0.039	7.19	3.86	>10.0
OVCAR-5	0.08	0.471	0.259	0.042	5.23	0.347	4.85
OVCAR-8	<0.01	0.326	0.124	<0.01	3.98	0.438	3.13
NCI/ADR-RES	<0.01	0.040	0.073	<0.01	0.317	0.059	1.47
SK-OV-3	<0.01	0.394	0.087	<0.01	2.49	0.626	1.79
Renal cancer							
786-0	<0.01	0.602	0.137	<0.01	5.84	1.06	2.44
A498	<0.01	0.040	0.029	<0.01	0.540	0.198	0.417
ACHN	<0.01	0.082	0.079	0.217	12.4	0.089	0.518
CAKI-1	<0.01	0.103	0.035	<0.01	0.492	0.047	0.482
RXF 393	<0.01	0.151	0.055	<0.01	1.30	0.148	0.551
SN12C	<0.01	0.779	0.269	<0.01	0.956	0.515	4.68
TK-10	<0.01	5.56	20.1	73.6	2.28	0.063	2.78
UO-31	<0.01	0.071	0.201	2.29	3.79	0.083	0.679
Prostate cancer							
PC-3	<0.01	0.062	0.105	<0.01	2.41	0.341	2.74
DU-145	<0.01	0.206	0.207	<0.01	1.30	0.333	1.07
Breast cancer							
MCF7	0.016	0.289	0.039	0.023	0.446	0.034	0.399
MDA-MB-231/ATCC	0.014	0.291	0.294	0.028	1.21	0.992	6.74
HS 578T	<0.01	0.133	0.092	<0.01	1.88	1.29	2.01
BT-549	<0.01	0.0978	0.109	0.029	0.950	12.2	3.45
T-47D	2.50	0.573	95.2	4.34	0.996	nd	1.18
MDA-MB-468	0.022	0.350	0.041	0.022	0.421	0.084	2.04

na: Not analyzed, nd: not determined, [a]GI_{50}: 50% growth inhibition, concentration of drug resulting in a 50% reduction in net cell growth as compared to cell numbers on day 0.

Table 2
Growth inhibition (GI_{50}/μM)[a] data for (*Z*)-indole-3-yl (**21**–**24**) and (*Z*)-benzo[*b*]furan-3-yl (**25**) cyanocombretastatin analogues.

Panel/cell line	**21**	**22**	**23**	**24**	**25**
	μM	μM	μM	μM	μM
Leukemia					
CCRF-CEM	0.058	2.74	0.042	0.064	1.41
HL-60(TB)	0.048	4.57	0.031	0.059	1.03
K-562	0.040	1.65	0.043	0.044	0.513
MOLT-4	0.131	3.99	0.049	0.198	3.82
RPMI-8226	0.231	3.96	0.065	0.241	2.47
SR	0.022	1.45	0.033	0.027	0.681
Lung cancer					
A549/ATCC	0.078	5.16	0.061	0.086	0.665
EKVX	0.596	18.5	0.478	0.485	na
HOP-62	0.082	8.69	0.273	0.133	6.98
HOP-92	1.01	5.26	0.068	0.083	3.02
NCI-H226	0.194	20.9	8.18	0.170	6.20
NCI-H23	0.133	7.19	0.256	0.101	4.58
NCI-H322M	nd	24.3	nd	0.044	19.1
NCI-H460	0.041	4.51	0.039	0.037	0.839
NCI-H522	0.037	3.05	0.027	0.086	0.261
Colon cancer					
COLO 205	0.474	5.31	0.047	0.051	0.449
HCC-2998	0.107	12.6	0.207	0.119	4.13
HCT-116	0.048	35.5	0.042	0.045	0.517
HCT-15	0.051	3.70	0.053	0.068	0.492
HT29	0.038	3.32	0.038	0.038	0.394
KM12	0.043	4.04	0.040	0.044	0.586
SW-620	0.047	3.53	0.044	0.046	0.504
CNS Cancer					
SF-268	2.54	18.9	0.078	2.14	4.79
SF-295	0.042	4.92	0.045	0.042	0.446
SF-539	0.099	8.42	0.052	0.071	0.442
SNB-19	0.076	24.2	0.062	0.089	3.63
SNB-75	0.042	6.04	0.034	0.043	0.769
U251	0.050	4.97	0.045	0.050	0.605
Melanoma					
LOX IMVI	0.075	5.32	0.078	0.074	0.993
MALME-3M	12.5	9.91	nd	5.85	0.868
M14	0.053	3.75	0.042	0.052	0.667
MDA-MB-435	0.024	3.95	0.020	0.027	0.278
SK-MEL-2	na	4.70	0.051	na	0.304
SK-MEL-28	0.090	6.25	0.081	0.092	1.61
SK-MEL-5	0.042	4.27	0.048	0.036	0.336
UACC-257	11.3	11.9	nd	10.7	nd
UACC-62	0.048	6.98	0.049	0.059	0.519
Ovarian cancer					
IGROV1	0.417	21.0	0.347	0.379	3.06
OVCAR-3	0.033	5.68	0.031	0.034	0.277
OVCAR-4	0.338	22.1	3.52	1.35	2.61
OVCAR-5	10.6	>100	0.197	0.516	3.33
OVCAR-8	0.121	7.38	0.103	0.148	2.90
NCI/ADR-RES	0.039	1.70	0.033	0.037	0.382
SK-OV-3	0.051	11.9	0.117	0.056	1.71
Renal cancer					
786-0	0.090	14.1	0.077	0.085	6.11
A498	0.035	3.36	0.035	0.025	0.458
ACHN	1.76	23.7	nd	1.66	1.94
CAKI-1	0.058	4.34	0.035	0.072	0.650
RXF 393	0.036	4.48	0.083	0.033	0.496
SN12C	0.699	8.10	0.077	0.715	2.17
TK-10	11.1	13.2	10.3	20.1	2.10
UO-31	1.41	14.3	0.663	1.26	2.89
Prostate cancer					
PC-3	0.054	7.85	0.075	0.054	1.84
DU-145	0.132	22.6	0.130	0.153	1.88
Breast cancer					
MCF7	0.034	3.10	0.041	0.036	0.376
MDA-MB-231/ATCC	0.245	7.18	0.644	0.299	1.71
HS 578T	0.131	12.9	0.611	0.124	2.03
BT-549	1.94	5.38	0.049	0.348	0.927
T-47D	0.058	6.83	nd	0.065	0.811
MDA-MB-468	0.041	na	0.051	0.035	0.237

na: Not analyzed, nd: not determined, [a]GI_{50}: 50% growth inhibition, concentration of drug resulting in a 50% reduction in net cell growth as compared to cell numbers on day 0.

ovary, renal, prostate, and breast cancer cell lines. The compounds were considered for progression to full five-concentration assay if they reduced the growth of cancer cells to 60% or more in at least eight of the 60 cell lines screened. The single dose results are expressed as the percent growth inhibition of treated cells at the test concentration of 10^{-5} M following 48 h of incubation. From the preliminary screens, compounds **8**, **9**, **11**–**13**, **15**, **17** and **21**–**25** were selected as leads for more comprehensive studies designed to determine GI_{50}, TGI and LC_{50} values, which represent the molar drug concentration required to cause 50% growth inhibition, total growth inhibition, and the concentration that kills 50% of the cells, respectively. The compounds were evaluated using five different concentrations at 10-fold dilutions (10^{-4} M, 10^{-5} M, 10^{-6} M, 10^{-7} M and 10^{-8} M) and incubations were carried out over 48 h exposure to drug. *Trans*-cyanostilbenes analogues which contained the 3,4,5-trimethoxyphenyl (**8**, **11**, **12**, **15**, **21**, **24** and **25**) and dimethoxyphenyl (**9**, **13**, **17**, **22** and **23**) moieties exhibited low micromolar level growth inhibition in subsequent five dose screening assays against all 60 human cancer cell lines in the panel. The growth inhibition results of the most potent of these compounds are presented in Tables 1 and 2. We hypothesized that the cytotoxic activity of these novel analogues was likely due to their interaction with the colchicine binding site on tubulin.

2.2.2. Indol-2-yl analogues

Compound **8** [(*Z*)-3-(1*H*-indol-2-yl)-2-(3,4,5-trimethoxyphenyl)acrylonitrile] exhibited GI_{50} values ranging from <0.01 μM to 1.16 μM in 95% of the cancer cell lines screened, and showed potent growth inhibition (GI_{50} = <0.01 μM) in 74% of the cancer cells in the 60-cell panel (Table 1).

The 3,4-dimethoxyphenyl acrylonitrile analog of **8**, compound **9**, which lacks the 5-methoxy group on the phenyl ring, also exhibited potent growth inhibition against 93% of the cancer cell lines in the panel, with GI_{50} values ranging from 0.021 to 0.779 μM, and afforded an average GI_{50} value of 0.80 μM against all the cancer cell lines in the panel (Table 1). This compound exhibited potent growth inhibition against MDA-MB-435 melanoma cancer cells with a GI_{50} = 0.021 μM (Table 1).

The introduction of an *N*-(4-cyanobenzyl) group into the structure of compound **8** afforded compound **11** [(*Z*)-4-((2-(2-cyano-2-(3,4,5-trimethoxyphenyl)vinyl)-1*H*-indol-1-yl)-methyl) benzonitrile], which exhibited GI_{50} values ranging from 0.024 μM to 0.672 μM in 95% of the cancer cell lines screened and showed potent growth inhibition properties in all five leukemia cell lines, with GI_{50} values in the range 0.031–0.274 μM. Compound **11** also showed potent growth inhibition against the MDA-MB-435 melanoma cell line (GI_{50} = 0.024 μM), and exhibited growth inhibition < 1 μM against 93% of the cancer cells in the 60-cell panel (Table 1).

2.2.3. Benzofuran-2-yl analogues

Substitution of the 2-indolyl moiety in compound **8** for a benzofuran-2-yl moiety afforded compound **12** [(*Z*)-3-(benzofuran-2-yl)-2-(3,4,5-trimethoxyphenyl)acrylonitrile], which exhibited good growth inhibition against all the cancer cells in the 60-cell panel with GI_{50} values ranging from <0.01 to 73.6 μM. This compound exhibited remarkably potent growth inhibition against 70% of the cancer cell lines screened with GI_{50} = <0.01 μM (Table 1).

Substitution of the 3,4,5-trimethoxyphenyl group in **12** for the 3,4-dimethoxyphenyl moiety afforded compound **13** [(*Z*)-3-(benzofuran-2-yl)-2-(3,4-dimethoxyphenyl)acrylonitrile], which exhibited good growth inhibition against 54% the cancer cells in the panel with GI_{50} ranging from 0.229 to 0.996 μM. This compound exhibited potent growth inhibition of MDA-MB-435 melanoma cancer cells with a GI_{50} value of 0.229 μM (Table 1). The average GI_{50} value of this compound against all the cancer cell lines screened was 2.59 μM.

2.2.4. Benzo[d]thiazol-2-yl analogues

The substitution of a benzofuran-2-yl moiety in compound **12** for a benzo[d]thiazol-2-yl moiety afforded compound **15** [(*Z*)-3-(benzo[*d*]thiazol-2-yl)-2-(3,4,5-trimethoxyphenyl)acrylonitrile], which exhibited potent growth inhibition against 94% of the cancer cells in the 60-cell panel, with GI_{50} ranging from 0.021 to 12.2 μM. The average GI_{50} value for this compound against all the cancer cell lines screened was 0.93 μM. This compound exhibited potent growth inhibition against 73% of the cancer cell lines screened with GI_{50} = <1 μM (Table 1) and exhibited potent growth inhibition against MDA-MB-435 melanoma cancer cells with a GI_{50} of 0.021 μM (Table 1).

Substitution of the 3,4,5-trimethoxyphenyl group in **15** for the 3,5-dimethoxyphenyl moiety afforded compound **17** [(*Z*)-3-(benzo[*d*]thiazol-2-yl)-2-(3,5-dimethoxyphenyl)acrylonitrile], which exhibited potent growth inhibition against 94% of the cancer cells in the 60-cell panel with GI_{50} ranging from 0.199 to 8.39 μM. The average GI_{50} value for this compound against all the cancer cells in the panel was 1.87 μM. This compound exhibited potent growth inhibition against only 38% of the cancer cell lines screened with GI_{50} = <1 μM (Table 2). This compound exhibited potent growth inhibition against MDA-MB-435 melanoma cancer cells with a GI_{50} value of 0.199 μM (Table 1).

2.2.5. Indol-3-yl analogues

The indol-3-yl analog (**21**) of compound **8** exhibited good growth inhibition in the 60-cell screen with GI_{50} values ranging from 0.022 μM to 12.5 μM against all the cancer cell lines screened. Compound **21** showed potent growth inhibition against SR leukemia cells (GI_{50} = 0.022 μM), and exhibited <1 μM growth inhibition against 83% of the cancer cell lines screened (Table 2).

The indol-3-yl analog (**22**) of compound **9** exhibited growth inhibition against all the cancer cell lines screened with GI_{50} values ranging from 1.45 μM to >100 μM (Table 2).

Replacement of the 3,4-dimethoxyphenyl group in compound **22** with a 3,5-dimethoxyphenyl moiety afforded compound **23** [(*Z*)-3-(1*H*-indol-3-yl)-2-(3,5-dimethoxyphenyl)acrylonitrile], which exhibited good growth inhibition against all the cells in the panel with GI_{50} values ranging from 0.020 μM to 10.3 μM. This compound showed potent growth inhibition against melanoma MDA-MB-435 cancer cells with a GI_{50} value of 0.02 μM. Compound **23** exhibited <1 μM growth inhibition against 85% of the cancer cell lines screened (Table 2).

Replacement of the indol-3-yl group in compound **21** with a 5-methoxyindol-3-yl moiety afforded compound **24** [(*Z*)-3-(5-methoxy-1*H*-indol-3-yl)-2-(3,4,5-trimethoxyphenyl)acrylonitrile], which exhibited good growth inhibition against all the cancer cells in the panel, with GI_{50} values ranging from 0.025 to 20.1 μM. This compound exhibited potent growth inhibition against A498 renal cancer cells with a GI_{50} value of 0.022 μM. Compound **24** exhibited <1 μM growth inhibition against 88% of the cancer cell screened (Table 2).

2.2.6. Benzofuran-3-yl analogues

Replacement of the indol-3-yl group in compound **21** with a benzofuran-3-yl moiety afforded compound **25** [(*Z*)-3-(benzofuran-3-yl)-2-(3,4,5-trimethoxyphenyl)acrylonitrile], which exhibited good growth inhibition against all the cancer cells in the panel, with GI_{50} values ranging from 0.237 to 19.1 μM. The average GI_{50} value of this compound against all the cancer cell lines screened was 1.99 μM. This compound exhibited potent growth inhibition against 52% of the cancer cell lines screened with GI_{50} values <1 μM (Table 2).

From structure-activity relationships (SAR) it is evident of that the heterocyclic series of *trans*-cyano CA-4 analogues containing benzo[*b*]thiophene-2-yl [11], indole-2-yl, benzofuran-2-yl and benzothiazole-2-yl moieties exhibited more growth inhibitory activity than the corresponding isomeric benzo[*b*]thiophene-3-yl, indole-3-yl, benzofuran-3-yl analogues. Also, analogues containing a 3,4,5-trimethoxyphenyl group generally exhibited better growth inhibition properties than analogues containing a 3,4-dimethoxyphenyl or 3,5-dimethoxyphenyl moiety. Importantly, introduction of a 2-benzo[*b*]thiophenyl or 2-indolyl heterocyclic moiety in place of the 3-fluoro-4-methoxyphenyl moiety of *trans*-cyano CA-4 [9] (Fig. 1, **III**) dramatically improved anti-cancer activity.

2.3. Anti-leukemic activity

Previously, we have reported on the synthesis of (*Z*)-benzo[*b*]thiophen-2-yl acrylonitriles (**29**–**31**) (Fig. 2) [11] as potent anti-cancer agents and we have evaluated the biological activity of these compounds against PC3 prostate cancer cell lines [11]. Compound **29** was also screened for its *in vitro* inhibitory activity on tubulin polymerization in these prostate cancer cells utilizing both an immunofluorescence assay and by using antibody against tubulin [11]. These benzo[*b*] thiophen-2-yl acrylonitrile compounds were also able to overcome P-glycoprotein (P-gp)-mediated resistance in PC3-DR prostate cancer cell lines and also exhibited a concentration-dependent anti-tubulin interaction in both PC3 and PC3-DR prostate cancer cells [11]. We have also reported that the thiophen-2-yl analogue **29** exhibits more potent growth inhibition than the isomeric thiophen-3-yl analogue **31** [11].

Compounds **29** and **30** both exhibited low nanomolar range growth inhibition (GI_{50} < 10 nM) against all six leukemia cell lines in the NCI 60 cell line panel [11]. These results indicate that (*Z*)-benzo[*b*]thiophene analog **29** is a potential anti-leukemic compound.

In the current study, the novel cyanocombretastatin heteroaromatic analogues **8**, **11**–**17**, **21**–**25** and the previously reported (*Z*)-benzo[*b*]thiophene CA-4 analogs **29**–**31** [11] were evaluated for their anti-leukemic activity against the MV4-11 AML cell line (Table 3). From these studies, analogues **8**, **12** and **29** were determined to be the most active compounds against this leukemia cell line.

Compound **29** was further screened against a panel of 12 different primary leukemia cell lines, and showed a dose-dependent toxicity against most of the cell lines tested (Fig. 3). The average LD_{50} value for the 12 different leukemia cell lines was 132 nM (range: 18.0–271 nM). Specifically, MV4-11 cells exhibited the most sensitivity to compound **29** (LD_{50} = 18 nM), whereas THP-1 and MLL-ENL cells were the most resistant cell line (LD_{50} = 227.0 and 271 nM, respectively) (Fig. 3).

We also tested the activity of **29** against primary blast crisis chronic myeloid leukemia (CML) cells and found that the response to **29** was also time-dependent (Fig. 4.). We observed that at 96 h more than 50% of the cells were apoptotic/dead after exposure to drug concentrations as low as 25 nM. We have also found that the activity of **29** was mediated via the activation of caspase cascades (MLG/HZ personal communication).

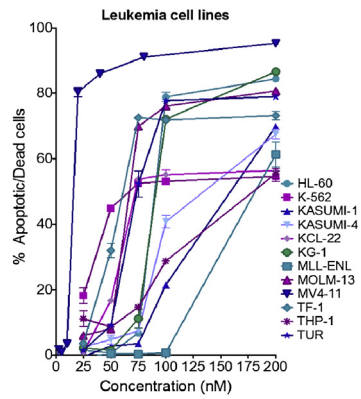

Cell Line	LD50 (nM)
HL-60	119.91
K-562	99.5
KASUMI-1	151.3
KASUMI-4	156.4
KCL-22	114.1
KG-1	112.8
MLL-ENL	270.7
MOLM-13	83.0
MV4-11	18.0
TF-1	79.5
THP-1	227.0
TUR	93.0

Fig. 3. Activity of compound **29** on 12 different leukemia cell lines.

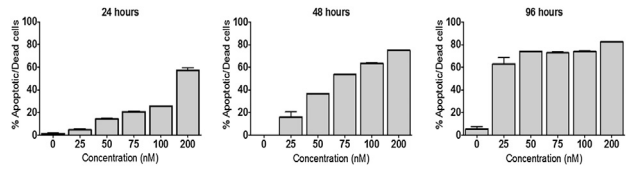

Fig. 4. Activity of compound **29** in a primary leukemia sample (blast crisis of chronic myeloid leukemia) at 24 h, 48 h and 96 h time-points.

2.4. Tubulin polymerization inhibition

Based upon the 60-cell screening results from the leukemia cell lines (Tables 1 and 2) and the data from the *in vitro* toxicity studies on cultured AML cells (Table 3), seven compounds: **8**, **12**, **21**, **23**, **25**, **29** and **31**, were screened for their *in vitro* inhibitory activity on tubulin polymerization utilizing both an immunofluorescence assay and by using antibody against tubulin (a marker for dynamic microtubules) (Fig. 5) [36].

MV4-11 cells were treated with the above seven compounds at doses of 25, 50 and 100 nM for 2 h and cell-based tubulin depolymerization assays performed. The polymerized tubulin in the pellet (P) and unpolymerized tubulin in the supernatant (S) were

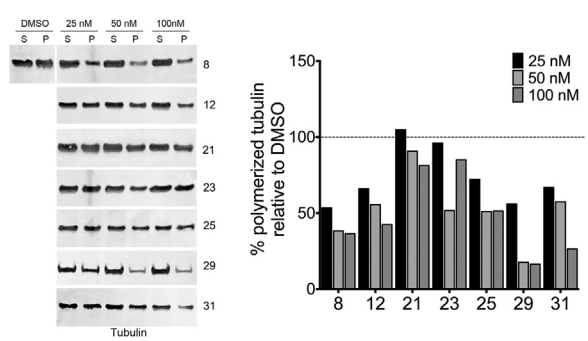

Fig. 5. Effect of *trans*-cyano CA-4 analogues **8**, **12**, **21**, **23**, **25**, **29** and **31** to inhibit tubulin polymerization in MV4-11 cells.

Table 3
Anti-leukemic activity (LD_{50}) of the most potent compounds against the MV4-11 AML cell line.

Compound	**8**	**11**	**12**	**13**	**14**	**15**	**16**	**17**
LD_{50} (μM)	0.044	0.369	0.047	>20	1.169	0.233	1.223	4.339
Compound	**21**	**22**	**23**	**24**	**25**	**29**	**30**	**31**
LD_{50} (μM)	0.565	>20	0.375	0.467	4.529	0.018	6.063	0.180

detected by immunoblotting using antibody against tubulin. Compounds **8**, **12**, and **29** all demonstrated >50% inhibition of tubulin polymerization at 50 nM concentration (Fig. 5).

2.5. Molecular docking

The binding modes of three of the most active compounds (**8**, **12**, and **29**) were determined at the colchicine binding site on tubulin using *in silico* molecular docking protocols. Chemical structures of the molecules were drawn using Marvin Sketch (ChemAxon). Atomic coordinates for the α,β-tubulin heterodimer were derived from the PDB file 1SA0 of the crystal structure of tubulin-colchicine complex. Input coordinate files for both the protein and the compounds were generated using the Dock Prep module in the UCSF-Chimera software.

Docking was performed using SwissDock (http://www.swissdock.ch/), which employs the EADock DSS algorithm to generate binding modes [37], estimate CHARMM energies [38], account for solvent effects using the FACTS implicit solvation model [39], and rank binding modes with the most favorable energies.

The top binding poses for the above three compounds at the colchicine-binding site of tubulin are shown in Fig. 6. The molecules are structurally very similar, differing only in the nature of the heterocyclic moiety in the molecule. All three of these heterocyclic moieties are 10-π electron bicyclic aromatic ring systems. The structural difference between the three compounds is due to the nature of the heteroatoms in the fused 5-membered ring of the heterocycle: i.e. indole (**8**), benzofuran (**12**), and benzothiophene (**29**). Thus, an additional interest in carrying out the molecular docking studies was to assess the effect of switching the heterocyclic moiety in these compounds on tubulin binding characteristics. None of the compounds make any polar contacts with tubulin residues. Instead, all of them occupy the same hydrophobic pocket at the α,β-interface where colchicine binds, and are stabilized through numerous van der Waals' interactions with residues from both subunits. Compound **8** is stabilized through Van der Waal's interactions with Gln11, Thr179 and and Val181 of α-tubulin, and Lys352, Val318, Cys241, Leu248, Lys254 of β-tubulin (Fig. 6A). The two compounds **12** and **29** show identical binding modes (Fig. 6B and C) that involve interactions with the same set of residues. In both cases, the ring containing the heteroatom (benzofuran in **12** and benzothiophene in **29**) is stabilized through Van der Waal's interactions with Asn101, Ser178, Thr179 and Val181 of α-tubulin (but not Gln11 as seen in compound **8**), and Asn258 and Lys352 of β-tubulin. However, the heteroatom-ring in the two compounds is rotated by 180° with respect to one another. The 3,4,5-trimethoxyphenyl moiety is stabilized by Cys241, Leu242, Leu248, Asp251, Lys254, Leu255, Met259, Val315 and Val318. Thus, the binding modes of compounds **12** and **29** are exactly superimposable on each other, except for their oppositely oriented heteroatoms ('O' in **12** and 'S' in **29**). The orientation of compound **8**, on the other hand, is not superimposable on those of **12** and **29**, although **8** also occupies the same binding pocket at the interface of α- and β-tubulin.

In summary, our molecular docking results were able to explain the trend in potencies observed for the three chosen compounds. This is further reflected in the free energy (ΔG) values of −8.12, −7.74 and −7.65, kcal/mol for compounds **29**, **12** and **8**, respectively.

3. Conclusions

Novel heterocyclic cyanocombretastatin A-4 analogues have been synthesized and evaluated for their anticancer activity against a panel of 60 human cancer cell lines. Compounds containing a trimethoxyphenyl moiety or a dimethoxyphenyl moiety showed potent growth inhibition, with GI_{50} values generally <1 μM against most of the cancer cell lines used, with **8** and **12** being the most potent compounds. The novel cyanocombretastatin heteroaromatic analogues **8**, **11**–**17**, **21**–**25** and the previously reported (*Z*)-benzo[*b*]thiophene CA-4 analogs **29**–**31** were evaluated for their anti-leukemic activity against the MV4-11 AML cell line. Compounds **8**, **12** and **29** also showed potent anti-leukemic activity against leukemia MV4-11 cell lines (LD_{50} = 44 nM, 47 nM, and 18 nM, respectively). The most active compound from the series, **29**, was also screened against a variety of 12 different leukemia cell lines and exhibited LD_{50} values <300 nM against all 12 leukemia cell lines. Compounds **8**, **12**, **21**, **23**, **25**, **29** and **31** were also screened for their *in vitro* inhibitory activity on tubulin polymerization in MV4-11 cells and compounds **8**, **12** and **29** all demonstrated >50% inhibition of tubulin polymerization at 50 nM concentrations. The binding modes of the three most active compounds, **8**, **12** and **29** at the colchicine binding site on tubulin have been investigated utilizing molecular docking studies are consistent with the rank potency of these compounds as inhibitors of tubulin polymerization. From the cell screening and molecular docking results, we consider compounds **8** and **29** as lead compounds in the development of new anticancer agents that target tubulin. Compounds **8** and **29** are

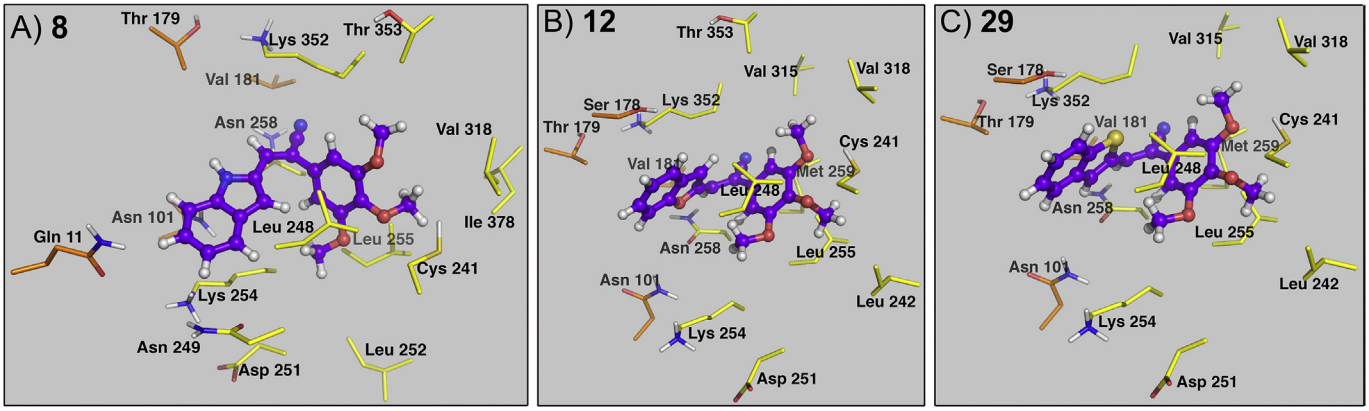

Fig. 6. Binding modes of A) compound **8**; B) compound **12**; C) compound **29**; at the colchicine-binding site of tubulin. The inhibitors are shown as *purple* ball-and-sticks and the tubulin residues are shown as *orange* (α-tubulin) and *yellow* (β-tubulin) sticks. (For interpretation of the references to color in this figure legend, the reader is referred to the web version of this article.)

considered lead compounds suitable for further development as anti-leukemic drugs.

4. Experimental section

4.1. Chemistry

Melting points were recorded on a Kofler hot-stage apparatus and are uncorrected. TLC controls were carried out on pre-coated silica gel plates (F 254 Merck). ^{1}H and ^{13}C NMR spectra were recorded on a Varian 400 MHz spectrometer equipped with a Linux workstation running on vNMRj software. All the spectra were phased, baseline was corrected where necessary, and solvent signals ($CDCl_3$) were used as reference for both ^{1}H and ^{13}C spectra. HRMS data was obtained on an Agilent 6210 LCTOF instrument operated in multimode.

4.2. Methodology for the in vitro 60 human cancer cell screen

The methodology for the anti-cancer screening assay was carried out as per the reported literature procedure [40], which is also available at http://dtp.nci.nih.gov/branches/btb/ivclsp.html http://dtp.nci.nih.gov/branches/btb/ivclsp.html.

4.3. Methodology for anti-leukemic activity determination

MV4-11 cells were cultured in Iscove's Modified Dulbecco's Media (IMDM) supplemented with 100 U/ml penicillin, 100 U/ml streptomycin, and 10% fetal bovine serum (Life technologies). Cells were seeded at 5 × 105/ml, and treated with the test compounds. At 24 and 48 h post treatment, cells were stained with annexin V-FITC (BD Biosciences) and 1 μg/ml 7-AAD (Life Technologies). Percent cell dead was determined by flow cytometry as the percent of annexin V+ cells. Data were analyzed using Flowjo 9.3.2 for Mac OS X (TreeStar). The cell death was represented relative to vehicle control (DMSO).

4.4. Methodology for blast crisis chronic myeloid leukemia analyses

Primary blast crisis chronic myeloid leukemia (CML) samples were obtained with informed consent and IRB approval from Weill Cornell Medical College. The cryopreserved primary samples were thawed and cultured as previously described [41]. Cells were treated with indicated doses of compound. At 48 h post treatment, cells were stained with CD45-APC-H7 (BD Biosciences), followed by annexin V-FITC and 7-AAD staining. Cell dead was determined by flow cytometry. The percent cell dead of treated cells is represented by percent of annexin V+ blasts normalized to DMSO control.

4.5. Tubulin polymerization inhibition assay

MV4-11 cells were treated with indicated doses of compounds for 2 h. Cells were then lysed in microtubule-stabilizing buffer (100 mM Pipes, 1 mM EGTA, 1 mM $MgSO_4$, 30% glycerol, 5% DMSO, 1 mM DTT, 0.02% NaN_3, 0.125% NP-40, pH 6.9) at 37 °C. Free tubulin (supernatants, S) and polymerized tubulin (pellets, P) were examined by immunoblotting using tubulin antibody. Both microtubule-stabilizing and microtubule-destabilizing drugs inhibit hypoxia-inducible factor-1 alpha accumulation and activity by disrupting microtubule function [42].

4.6. General synthetic procedure: synthesis of (Z)-heterocyclic cyanocombretastatins (**8**–**17** and **21**–**27**)

A mixture of carbaldehyde (1.0 mole) and the appropriate substituted phenylacetonitrile (1.1 mole) in 5% sodium methoxide/methanol was heated under reflux for 3–6 h. The resulting solution was cooled to room temperature and poured into ice-cold water to afford a crude yellow solid. The solid was filtered off, washed with water, and finally washed with cold methanol. The obtained crude solid was recrystallized from methanol to afford the desired condensation product as a pure yellow crystalline solid.

4.6.1. (Z)-3-(1H-indol-2-yl)-2-(3,4,5-trimethoxyphenyl)acrylonitrile (**8**)

mp: 147–148 °C, ^{1}H NMR (400 MHz, $CDCl_3$): δ 3.83 (s, 6H), 3.93 (s, 3H), 6.73 (s, 2H), 6.77 (s, 1H), 7.08–7.25 (m, 4H), 7.57 (d, $J = 8.0$ Hz, 1H), 7.90 (brs, 1H, NH) ppm; ^{13}C NMR (100 MHz, $CDCl_3$): δ 56.23, 60.92, 102.78, 105.90, 111.54, 111.79, 112.73, 119.88, 120.97, 121.11, 121.48, 121.74, 127.37, 129.14, 130.67, 130.92, 132.26, 138.10, 138.99, 153.69 ppm. HRMS (ESI) *m/z* calcd for $C_{20}H_{19}N_2O_3$ $[M+H]^+$ 335.1390; Found 335.1399.

4.6.2. (Z)-2-(3,4-Dimethoxyphenyl)-3-(1H-indol-2-yl)acryloni-trile (**9**)

mp: 170–172 °C, ^{1}H NMR (400 MHz, $CDCl_3$): δ 3.92 (s, 3H), 3.97 (s, 3H), 6.90 (s, 1H), 6.92 (s, 1H), 7.11–7.16 (m, 1H), 7.22 (dd, $J = 2$, 8.4 Hz, 1H), 7.29–7.41 (m 1H), 7.42–7.44 (m, 2H), 7.62 (d, $J = 8.4$ Hz, 1H), 9.47 (brs, 1H, NH) ppm; ^{13}C NMR (100 MHz, $CDCl_3$): δ 56.04, 56.06, 105.89, 108.14, 111.60, 112.11, 118.57, 119.98, 120.94, 121.49, 125.36, 126.34, 127.41, 129.56, 132.52, 137.98, 149.42, 149.95 ppm. HRMS (ESI) *m/z* calcd for $C_{19}H_{17}N_2O_2$ $[M+H]^+$ 305.1285; Found 305.1276.

4.6.3. (Z)-2-(3,5-Dimethoxyphenyl)-3-(1H-indol-2-yl)acrylonitrile (**10**)

mp: 195–197 °C, ^{1}H NMR (400 MHz, $CDCl_3$): δ 3.84 (s, 6H), 6.46 (t, $J = 2.0$ Hz, 1H), 6.77 (d, $J = 2.4$ Hz, 2H), 6.94 (d, $J = 2$ Hz, 1H), 7.12 (t, $J = 8.4$ Hz, 1H), 7.29–7.33 (m, 1H), 7.42 (d, $J = 8.8$ Hz, 1H), 7.50 (s, 1H), 7.62 (d, $J = 7.6$ Hz, 1H), 9.48 (brs, 1H, NH) ppm. ^{13}C NMR (100 MHz, $CDCl_3$): δ 55.54, 100.96, 103.70, 105.84, 111.70, 113.06, 119.85, 121.03, 121.66, 125.69, 127.34, 131.62, 132.22, 135.45, 138.17, 161.31 ppm. HRMS (ESI) *m/z* calcd for $C_{19}H_{17}N_2O_2$ $[M+H]^+$ 305.1285; Found 305.1290.

4.6.4. (Z)-4-((2-(2-Cyano-2-(3,5-dimethoxyphenyl)vinyl)-1H-indo1-yl)methyl)benzonitrile (**11**)

mp: 190–192 °C, ^{1}H NMR (400 MHz, $CDCl_3$): δ 3.84 (s, 6H), 3.85 (s, 3H), 5.51 (s, 2H, $-CH_2$), 6.64 (s, 2H), 7.11 (d, $J = 8$ Hz, 2H), 7.18–7.29 (m, 4H), 7.58 (d, $J = 8.4$ Hz, 2H), 7.74 (d, $J = 8$ Hz, 1H), 7.79 (s, 1H) ppm; ^{13}C NMR (100 MHz, $CDCl_3$): δ 46.33, 56.27, 60.99, 103.25, 107.35, 107.33, 109.27, 110.92, 111.98, 118.07, 118.14, 121.44, 122.50, 125.11, 126.61, 127.58, 127.88, 129.72, 132.73, 132.88, 138.23, 142.59, 153.62 ppm. HRMS (ESI) *m/z* calcd for $C_{28}H_{24}N_3O_3$ $[M+H]^+$ 450.1826; Found 450.1821.

4.6.5. (Z)-3-(Benzofuran-2-yl)-2-(3,4,5-trimethoxyphenyl)acrylonitrile (**12**)

mp: 102–104 °C, ^{1}H NMR (400 MHz, $CDCl_3$): δ 3.90 (s, 3H), 3.91 (s, 6H), 6.89 (s, 2H), 7.26–7.31 (m, 1H), 7.36–7.40 (m, 1H), 7.41 (s, 1H), 7.50 (s, 1H), 7.53 (dd, $J = 1.2$, 10 Hz, 1H), 7.63–7.65 (m, 1H) ppm; ^{13}C NMR (100 MHz, $CDCl_3$): δ 56.53, 61.25, 103.30, 110.89, 111.10, 111.71, 117.60, 122.16, 123.81, 126.94, 127.66, 128.29, 129.17, 139.50, 151.21, 153.68, 155.20 ppm. HRMS (ESI) *m/z* calcd for $C_{20}H_{18}NO_4$ $[M+H]^+$ 336.1230; Found 336.1224.

4.6.6. (Z)-3-(Benzofuran-2-yl)-2-(3,4-dimethoxyphenyl)acrylonitrile (**13**)

mp: 111–113 °C, ^{1}H NMR (400 MHz, $CDCl_3$): δ 3.91 (s, 3H), 3.95 (s, 3H), 6.89 (d, $J = 8$ Hz, 2H), 7.14 (d, $J = 2.4$ Hz, 1H), 7.24–7.29 (m, 1H),

7.34–7.38 (m, 2H), 7.45 (s, 1H), 7.51 (d, J = 8.4 Hz, 1H), 7.60 (d, J = 7.6 Hz, 1H) ppm; ^{13}C NMR (100 MHz, $CDCl_3$): δ 56.17, 108.50, 110.43, 110.87, 111.45, 111.64, 117.70, 119.33, 122.05, 123.72, 126.36, 126.45, 126.70, 128.40, 149.52, 150.56, 151.54, 155.18 ppm. HRMS (ESI) m/z calcd for $C_{19}H_{16}NO_3$ $[M+H]^+$ 306.1125; Found 306.1131.

*4.6.7. (Z)-3-(Benzofuran-2-yl)-2-(3,5-dimethoxyphenyl)acrylonitrile (**14**)*

mp: 142–144 °C, ^{1}H NMR (400 MHz, $CDCl_3$): δ 3.84 (s, 6H), 6.49 (s, 1H), 6.81 (d, J = 2.0 Hz, 2H), 7.25 (t, J = 7.6 Hz, 1H), 7.37 (t, J = 7.6 Hz, 1H), 7.45 (s, 1H), 7.49 (s, H), 7.53 (d, J = 8.8 Hz, 1H), 7.62 (d, J = 8.0 Hz, 1H) ppm. ^{13}C NMR (100 MHz, $CDCl_3$): δ 55.54, 101.65, 104.08, 110.79, 111.36, 111.63, 117.41, 122.08, 123.66, 126.89, 128.15, 128.48, 135.43, 151.07, 155.22, 161.27 ppm. HRMS (ESI) m/z calcd for $C_{19}H_{16}NO_3$ $[M+H]^+$ 306.1125 Found 306.1126.

*4.6.8. (Z)-3-(Benzo[d]thiazol-2-yl)-2-(3,4,5-trimethoxyphenyl) acrylonitrile (**15**)*

mp: 110–111 °C, ^{1}H NMR (400 MHz, $CDCl_3$): δ 3.90 (s, 3H), 3.93 (s, 6H), 6.98 (s, 2H), 7.50–7.57 (m, 2H), 7.95–8.00 (m, 2H), 8.10 (d, J = 7.6 Hz, 1H) ppm; ^{13}C NMR (100 MHz, $CDCl_3$): δ 56.33, 61.0, 103.74, 110.0, 116.74, 116.97, 121.85, 123.88, 126.98, 127.05, 128.11, 133.82, 135.49, 140.37, 140.57, 152.51, 153.72, 161.33 ppm. HRMS (ESI) m/z calcd for $C_{19}H_{17}N_2O_3S$ $[M+H]^+$ 353.0960; Found 353.0968.

*4.6.9. (Z)-3-(Benzo[d]thiazol-2-yl)-2-(3,4-dimethoxyphenyl)acrylonitrile (**16**)*

mp: 130–131 °C, ^{1}H NMR (400 MHz, $CDCl_3$): δ 3.94 (s, 3H), 3.95 (s, 3H), 6.93 (d, J = 8 Hz, 1H), 7.22 (s, 1H), 7.38 (d, J = 8 Hz, 1H), 7.48–7.55 (m, 2H), 7.91–7.96 (m, 2H), 8.08 (d, J = 8 Hz, 1H) ppm; ^{13}C NMR (100 MHz, $CDCl_3$): δ 56.08, 56.09, 108.39, 111.34, 116.79, 117.19, 120.47, 121.83, 123.59, 125.39, 126.88, 127.08, 131.90, 135.22, 149.58, 151.46, 152.02, 161.75 ppm. HRMS (ESI) m/z calcd for $C_{18}H_{15}N_2O_2S$ $[M+H]^+$ 323.0854; Found 323.0842.

*4.6.10. (Z)-3-(Benzo[d]thiazol-2-yl)-2-(3,5-dimethoxyphenyl)-acrylonitrile (**17**)*

mp: 149–151 °C, ^{1}H NMR (400 MHz, $CDCl_3$): δ 3.84 (s, 6H), 6.55 (s, 1H), 6.89 (s, 2H), 7.50–7.57 (m, 2H), 7.95–7.97 (d, J = 8 Hz, 1H), 8.04 (s, 1H), 8.11 (d, J = 8 Hz, 1H) ppm. ^{13}C NMR (100 MHz, $CDCl_3$): δ 55.60, 103.01, 104.55, 116.67, 117.32, 121.87, 123.86, 127.09, 127.14, 134.54, 134.58, 135.45, 152.15, 161.29, 161.37 ppm. HRMS (ESI) m/z calcd for $C_{18}H_{15}N_2O_2S$ $[M+H]^+$ 323.0849; Found 323.0850.

*4.6.11. (Z)-3-(1H-Indol-3-yl)-2-(3,4,5-trimethoxyphenyl)acrylonitrile (**21**)*

mp:178–180 °C, ^{1}H NMR (400 MHz, $CDCl_3$): δ 3.89 (s, 3H), 3.95 (s, 6H), 6.87 (s, 2H), 7.24–7.31 (m, 2H), 7.45 (d, J = 7.6 Hz, 1H), 7.77 (s, 1H), 7.78 (s, 1H), 8.42 (d, J = 2.8 Hz, 1H), 8.94 (brs, 1H, NH) ppm; ^{13}C NMR (100 MHz, $CDCl_3$): δ 56.32, 61.02, 102.79, 104.99, 111.77, 111.88, 117.95, 120.01, 121.27, 123.46, 126.25, 127.22, 130.71, 133.13, 135.54, 138.24, 153.58 ppm. HRMS (ESI) m/z calcd for $C_{20}H_{19}N_2O_3$ $[M+H]^+$ 335.1390; Found 335.1387.

*4.6.12. (Z)-2-(3,4-Dimethoxyphenyl)-3-(1H-indol-3-yl)acrylonitrile (**22**)*

mp: 170–172 °C, ^{1}H NMR (400 MHz, $CDCl_3$): δ 3.92 (s, 3H, $-OCH_3$), 3.97 (s, 3H, $-OCH_3$), 6.91 (d, J = 8.4 Hz, 1H), 7.15 (s, 1H), 7.24–7.21 (m, 3H), 7.44 (d, J = 7.6 Hz, 1H), 7.75 (s, 1H), 7.78 (s, 1H), 8.40 (s, 1H), 8.75 (brs, 1H, NH) ppm; ^{13}C NMR (100 MHz, $CDCl_3$): δ 55.97, 56.12, 104.92, 108.44, 108.55, 111.47, 111.73, 111.89, 117.90, 118.22, 120.14, 121.08, 121.24, 123.31, 125.90, 127.24, 127.83, 131.89, 135.53, 149.24 ppm. HRMS (ESI) m/z calcd for $C_{19}H_{17}N_2O_2$ $[M+H]^+$ 305.1285; Found 305.1278.

*4.6.13. (Z)-2-(3,5-Dimethoxyphenyl)-3-(1H-indol-3-yl)acrylonitrile (**23**)*

mp: 190–192 °C, ^{1}H NMR (400 MHz, $CDCl_3$): δ 3.86 (s, 6H), 6.45 (s, 1H), 6.82 (s, 2H), 7.25–7.29 (m, 2H), 7.44 (d, J = 8.0 Hz, 1H), 7.75 (d, J = 7.2 Hz, 1H), 7.87 (s, 1H), 8.44 (s, 1H), 8.83 (brs, 1H, NH) ppm; ^{13}C NMR (100 MHz, $CDCl_3$): δ 55.52, 100.10, 103.67, 111.79, 118.00, 119.95, 121.38, 123.50, 126.40, 127.28, 133.78, 135.45, 136.84, 161.21 ppm. HRMS (ESI) m/z calcd for $C_{19}H_{17}N_2O_2$ $[M+H]^+$ 305.1285; Found 305.1297.

*4.6.14. (Z)-3-(5-Methoxy-1H-indol-3-yl)-2-(3,4,5-trimethoxyphenyl)acrylonitrile (**24**)*

mp: 183–185 °C, ^{1}H NMR (400 MHz, $CDCl_3$): δ 3.88 (s, 3H, $-OCH_3$), 3.89 (s, 3H, $-OCH_3$), 3.94 (s, 6H, $-OCH_3$), 6.85 (s, 2H), 6.93 (d, J = 8.8 Hz, 1H), 7.18 (s, 1H), 7.33 (d, J = 8.4 Hz, 1H), 7.69 (s, 1H), 8.38 (s, 1H), 8.60 (brs, 1H, NH) ppm; ^{13}C NMR (100 MHz, $CDCl_3$): δ 55.98, 56.37, 61.00, 100.47, 102.95, 104.74, 111.72, 112.52, 113.21, 120.02, 126.78, 127.93, 130.52, 130.80, 133.17, 153.60, 155.39 ppm. HRMS (ESI) m/z calcd for $C_{21}H_{21}N_2O_4$ $[M+H]^+$ 365.1496; Found 365.1502.

*4.6.15. (Z)-3-(Benzofuran-3-yl)-2-(3,4,5-trimethoxyphenyl)acrylonitrile (**25**)*

mp: 144–146 °C, ^{1}H NMR (400 MHz, $CDCl_3$): δ 3.91 (s, 3H), 3.96 (s, 6H), 6.89 (s, 2H), 7.37–7.41 (m, 2H), 7.55 (s, 1H), 7.57 (d, J = 8.4 Hz, 1H), 7.72 (d, J = 7.6 Hz, 1H), 8.67 (s, 1H) ppm; ^{13}C NMR (100 MHz, $CDCl_3$): δ 56.82, 61.47, 103.72, 112.10, 112.48, 116.53, 119.01, 119.37, 123.97, 125.99, 126.67, 129.83, 129.98, 139.70, 146.35, 154.14, 155.35 ppm. HRMS (ESI) m/z calcd for $C_{20}H_{18}NO_4$ $[M+H]^+$ 336.1236; Found 336.1218.

*4.6.16. (Z)-3-(Benzofuran-3-yl)-2-(3,4-dimethoxyphenyl)acry-lo nitrile (**26**)*

mp: 135–137 °C, ^{1}H NMR (400 MHz, $CDCl_3$): δ 3.92 (s, 3H), 3.96 (s, 3H), 6.90 (d, J = 8.8 Hz, 1H), 7.13 (d, J = 2.4 Hz, 1H), 7.24 (dd, J = 2.4, 8.4 Hz, 1H), 7.33–7.40 (m, 2H), 7.49 (s, 1H), 7.54 (d, J = 8.4 Hz, 1H), 8.62 (s, 1H) ppm; ^{13}C NMR (100 MHz, $CDCl_3$): δ 56.04, 56.08, 108.64, 111.38, 111.48, 111.96, 116.18, 118.66, 118.82, 118.92, 123.42, 125.42, 126.32, 126.57, 128.11, 145.55, 149.38, 150.13, 154.84 ppm. HRMS (ESI) m/z calcd for $C_{19}H_{16}NO_3$ $[M+H]^+$ 306.1125; Found 306.1126.

*4.6.17. (Z)-3-(Benzofuran-3-yl)-2-(3,5-dimethoxyphenyl)acry lo nitrile (**27**)*

mp:121–123 °C, ^{1}H NMR (400 MHz, $CDCl_3$): δ 3.86 (s, 6H), 6.50 (s, 1H), 6.81 (s, 2H), 7.34–7.42 (m, 2H), 7.56 (d, J = 7.2 Hz, 1H), 7.62 (s, 1H), 7.69 (d, J = 8 Hz, 1H), 8.68 (s, 1H); ppm; ^{13}C NMR (100 MHz, $CDCl_3$): 55.54, 101.06, 104.11, 111.48, 111.98, 116.03, 118.50, 118.91, 123.57, 125.52, 126.24, 130.40, 135.65, 146.12, 154.85, 161.29 ppm. HRMS (ESI) m/z calcd for $C_{19}H_{16}NO_3$ $[M+H]^+$ 306.1125; Found 306.1133.

Acknowledgments

We are grateful to NCI/NIH (Grant Number CA 140409) and to the Arkansas Research Alliance (ARA) for financial support, M.L.G is funded by the US National Institutes of Health (NIH) through the NIH Director's New Innovator Award Program, 1 DP2 OD007399-01 and to the NCI Developmental Therapeutic Program (DTP) for screening data.

Appendix A. Supplementary data

Supplementary data related to this article can be found at http://dx.doi.org/10.1016/j.ejmech.2014.12.050.

References

[1] G.R. Pettit, S.B. Singh, E. Hamel, C.M. Lin, D.S. Alberts, D. Garcia-Kendall, Isolation and structure of the strong cell growth and tubulin inhibitor combretastatin A-4, Experientia 45 (1989) 209–211.

[2] G.R. Pettit, G.M. Cragg, D.L. Herald, J.M. Schmidt, P. Lobavanijaya, G.M. Cragg, D.L. Herald, J.M. Schmidt, P. Lobavanijaya, Isolation & structure of combretastatin, Can. J. Chem. 60 (1982) 1347–1376.

[3] C.M. Lin, S.B. Singh, P.S. Chu, R.O. Dempcy, J.M. Schmidt, G.R. Pettit, E. Hamel, Interactions of tubulin with potent natural and synthetic analogs of the antimitotic agent combretastatin: a structure-activity study, Mol. Pharmacol. 34 (1988) 200–208.

[4] M. Cushman, D. Nagarathnam, D. Gopal, A.K. Chakraborti, C.M. Lin, E. Hamel, Synthesis and evaluation of stilbene and dihydrostilbene derivatives as potential anticancer agents that inhibit tubulin polymerization, J. Med. Chem. 34 (1991) 2579–2588.

[5] K.W. Wood, W.D. Cornwell, J.R. Jackson, Past and future of the mitotic spindle as an oncology target, Curr. Opin. Pharmacol. 1 (2001) 370–377.

[6] M. Cushman, D. Nagarathnam, D. Gopal, H.M. He, C.M. Lin, E. Hamel, Synthesis and evaluation of analogues of (Z)-1-(4-methoxyphenyl)-2-(3,4,5-trimethoxyphenyl)ethene as potential cytotoxic and antimitotic agents, J. Med. Chem. 35 (1992) 2293–2306.

[7] A.T. McGown, B.W. Fox, Structural and biochemical comparison of the antimitotic agents colchicine, combretastatin A4 and amphethinile, Anticancer Drug Des. 3 (1989) 249–254.

[8] K. Ohsumi, R. Nakagawa, Y. Fukuda, T. Hatanaka, Y. Morinaga, Y. Nihei, K. Ohishi, Y. Suga, Y. Akiyama, T. Tsuji, Novel combretastatin analogues effective against murine solid tumors: design and structure-activity relationships, J. Med. Chem. 41 (1998) 3022–3032.

[9] P.H. Jalily, J.A. Hadfield, N. Hirst, S.B. Rossington, Novel cyanocombretastatins as potent tubulin polymerisation inhibitors, Bioorg. Med. Chem. Lett. 22 (2012) 6731–6734.

[10] A.B. Maya, C. Perez-Melero, C. Mateo, D. Alonso, J.L. Fernandez, C. Gajate, F. Mollinedo, R. Pelaez, E. Caballero, M. Medarde, Further naphthylcombretastatins. An investigation on the role of the naphthalene moiety, J. Med. Chem. 48 (2005) 556–568.

[11] N.R. Penthala, V.N. Sonar, J. Horn, M. Leggas, J.S. Yadlapalli, P.A. Crooks, Synthesis and evaluation of a series of benzothiophene acrylonitrile analogs as anticancer agents, Medchemcomm 4 (2013) 1073–1078.

[12] N.R. Penthala, V. Janganati, S. Bommagani, P.A. Crooks, Synthesis and evaluation of a series of quinolinyl trans-cyanostilbene analogs as anticancer agents, Medchemcomm 5 (2014) 886–890.

[13] X.F. Wang, S.B. Wang, E. Ohkoshi, L.T. Wang, E. Hamel, K. Qian, S.L. Morris-Natschke, K.H. Lee, L. Xie, N-aryl-6-methoxy-1,2,3,4-tetrahydroquinolines: a novel class of antitumor agents targeting the colchicine site on tubulin, Eur. J. Med. Chem. 67 (2013) 196–207.

[14] L.H. Zhang, L. Wu, H.K. Raymon, R.S. Chen, L. Corral, M.A. Shirley, R.K. Narla, J. Gamez, G.W. Muller, D.I. Stirling, J.B. Bartlett, P.H. Schafer, F. Payvandi, The synthetic compound CC-5079 is a potent inhibitor of tubulin polymerization and tumor necrosis factor-alpha production with antitumor activity, Cancer Res. 66 (2006) 951–959.

[15] A. Loupy, M. Pellet, A. Petit, G. Vo-Thanh, Solvent-free condensation of phenylacetonitrile and nonanenitrile with 4-methoxybenzaldehyde: optimization and mechanistic studies, Org. Biomol. Chem. 3 (2005) 1534–1540.

[16] F. Saczewski, P. Reszka, M. Gdaniec, R. Grunert, P.J. Bednarski, Synthesis, X-ray crystal structures, stabilities, and in vitro cytotoxic activities of new heteroarylacrylonitriles, J. Med. Chem. 47 (2004) 3438–3449.

[17] T. Graening, H.G. Schmalz, Total syntheses of colchicine in comparison: a journey through 50 years of synthetic organic chemistry, Angew. Chem. Int. Ed. Engl. 43 (2004) 3230–3256.

[18] G.R. Pettit, B. Toki, D.L. Herald, P. Verdier-Pinard, M.R. Boyd, E. Hamel, R.K. Pettit, Antineoplastic agents. 379. Synthesis of phenstatin phosphate, J. Med. Chem. 41 (1998) 1688–1695.

[19] N.H. Nam, Combretastatin A-4 analogues as antimitotic antitumor agents, Curr. Med. Chem. 10 (2003) 1697–1722.

[20] R.B. Ravelli, B. Gigant, P.A. Curmi, I. Jourdain, S. Lachkar, A. Sobel, M. Knossow, Insight into tubulin regulation from a complex with colchicine and a stathmin-like domain, Nature 428 (2004) 198–202.

[21] T.L. Nguyen, C. McGrath, A.R. Hermone, J.C. Burnett, D.W. Zaharevitz, B.W. Day, P. Wipf, E. Hamel, R. Gussio, A common pharmacophore for a diverse set of colchicine site inhibitors using a structure-based approach, J. Med. Chem. 48 (2005) 6107–6116.

[22] E. Rasolofonjatovo, O. Provot, A. Hamze, J. Rodrigo, J. Bignon, J. Wdzieczak-Bakala, D. Desravines, J. Dubois, J.D. Brion, M. Alami, Conformationnally restricted naphthalene derivatives type isocombretastatin A-4 and isoerianin analogues: synthesis, cytotoxicity and antitubulin activity, Eur. J. Med. Chem. 52 (2012) 22–32.

[23] Y. Hu, X. Lu, K. Chen, R. Yan, Q.S. Li, H.L. Zhu, Design, synthesis, biological evaluation and molecular modeling of 1,3,4-oxadiazoline analogs of combretastatin-A4 as novel antitubulin agents, Bioorg. Med. Chem. 20 (2012) 903–909.

[24] K. Gaukroger, J.A. Hadfield, N.J. Lawrence, S. Nolan, A.T. McGown, Structural requirements for the interaction of combretastatins with tubulin: how important is the trimethoxy unit? Org. Biomol. Chem. 1 (2003) 3033–3037.

[25] G.C. Tron, T. Pirali, G. Sorba, F. Pagliai, S. Busacca, A.A. Genazzani, Medicinal chemistry of combretastatin A4: present and future directions, J. Med. Chem. 49 (2006) 3033–3044.

[26] M. Banimustafa, A. Kheirollahi, M. Safavi, S. Kabudanian Ardestani, H. Aryapour, A. Foroumadi, S. Emami, Synthesis and biological evaluation of 3-(trimethoxyphenyl)-2(3H)-thiazole thiones as combretastatin analogs, Eur. J. Med. Chem. 70 (2013) 692–702.

[27] J. Zhou, J. Jin, Y. Zhang, Y. Yin, X. Chen, B. Xu, Synthesis and antiproliferative evaluation of novel benzoimidazole-contained oxazole-bridged analogs of combretastatin A-4, Eur. J. Med. Chem. 68 (2013) 222–232.

[28] C. Vilanova, S. Torijano-Gutierrez, S. Diaz-Oltra, J. Murga, E. Falomir, M. Carda, J. Alberto Marco, Design and synthesis of pironetin analogue/combretastatin A-4 hybrids containing a 1,2,3-triazole ring and evaluation of their cytotoxic activity, Eur. J. Med. Chem. 87C (2014) 125–130.

[29] Q. Guan, F. Yang, D. Guo, J. Xu, M. Jiang, C. Liu, K. Bao, Y. Wu, W. Zhang, Synthesis and biological evaluation of novel 3,4-diaryl-1,2,5-selenadiazol analogues of combretastatin A-4, Eur. J. Med. Chem. 87C (2014) 1–9.

[30] A. Chaudhary, S.N. Pandeya, P. Kumar, P.P. Sharma, S. Gupta, N. Soni, K.K. Verma, G. Bhardwaj, Combretastatin a-4 analogs as anticancer agents, Mini Rev. Med. Chem. 7 (2007) 1186–1205.

[31] J.A. Woods, J.A. Hadfield, G.R. Pettit, B.W. Fox, A.T. McGown, The interaction with tubulin of a series of stilbenes based on combretastatin A-4, Br. J. Cancer 71 (1995) 705–711.

[32] G.C. Tron, F. Pagliai, E. Del Grosso, A.A. Genazzani, G. Sorba, Synthesis and cytotoxic evaluation of combretafurazans, J. Med. Chem. 48 (2005) 3260–3268.

[33] C. Perez-Melero, A.B. Maya, B. del Rey, R. Pelaez, E. Caballero, M. Medarde, A new family of quinoline and quinoxaline analogues of combretastatins, Bioorg. Med. Chem. Lett. 14 (2004) 3771–3774.

[34] N.R. Penthala, S. Parkin, P.A. Crooks, (Z)-3-(1-Benzofuran-2-yl)-2-(3,4,5-trimeth-oxy-phen-yl)acrylonitrile, Acta Crystallographica. E Struct. Rep. Online 68 (2012) o731.

[35] N.R. Penthala, S. Parkin, P.A. Crooks, (Z)-3-(1H-Indol-3-yl)-2-(3,4,5-trimethoxy-phen-yl)acrylonitrile, Acta Crystallographica. E Struct. Rep. Online 68 (2012) o729.

[36] P.W. Baas, M.M. Black, Individual microtubules in the axon consist of domains that differ in both composition and stability, J. Cell Biol. 111 (1990) 495–509.

[37] A. Grosdidier, V. Zoete, O. Michielin, SwissDock, a protein-small molecule docking web service based on EADock DSS, Nucleic Acids Res. 39 (2011) W270–W277.

[38] B.R. Brooks, C.L. Brooks 3rd, A.D. Mackerell Jr., L. Nilsson, R.J. Petrella, B. Roux, Y. Won, G. Archontis, C. Bartels, S. Boresch, A. Caflisch, L. Caves, Q. Cui, A.R. Dinner, M. Feig, S. Fischer, J. Gao, M. Hodoscek, W. Im, K. Kuczera, T. Lazaridis, J. Ma, V. Ovchinnikov, E. Paci, R.W. Pastor, C.B. Post, J.Z. Pu, M. Schaefer, B. Tidor, R.M. Venable, H.L. Woodcock, X. Wu, W. Yang, D.M. York, M. Karplus, CHARMM: the biomolecular simulation program, J. Comput. Chem. 30 (2009) 1545–1614.

[39] U. Haberthur, A. Caflisch, FACTS: fast analytical continuum treatment of solvation, J. Comput. Chem. 29 (2008) 701–715.

[40] L.V. Rubinstein, R.H. Shoemaker, K.D. Paull, R.M. Simon, S. Tosini, P. Skehan, D.A. Scudiero, A. Monks, M.R. Boyd, Comparison of in vitro anticancer-drug-screening data generated with a tetrazolium assay versus a protein assay against a diverse panel of human tumor cell lines, J. Natl. Cancer Inst. 82 (1990) 1113–1118.

[41] M.L. Guzman, R.M. Rossi, S. Neelakantan, X. Li, C.A. Corbett, D.C. Hassane, M.W. Becker, J.M. Bennett, E. Sullivan, J.L. Lachowicz, A. Vaughan, C.J. Sweeney, W. Matthews, M. Carroll, J.L. Liesveld, P.A. Crooks, C.T. Jordan, An orally bioavailable parthenolide analog selectively eradicates acute myelogenous leukemia stem and progenitor cells, Blood 110 (2007) 4427–4435.

[42] D. Escuin, E.R. Kline, P. Giannakakou, Both microtubule-stabilizing and microtubule-destabilizing drugs inhibit hypoxia-inducible factor-1alpha accumulation and activity by disrupting microtubule function, Cancer Res. 65 (2005) 9021–9028.